Comparing the Brushless DFIM to other Generator Systems for Wind Turbine Drive-Trains

Strous, Tim; Shipurkar, Udai; Polinder, Henk; Ferreira, Bram

DOI
10.1088/1742-6596/753/11/112014

Publication date
2016

Document Version
Final published version

Published in
Journal of Physics: Conference Series

Comparing the Brushless DFIM to other Generator Systems for Wind Turbine Drive-Trains

2016 J. Phys.: Conf. Ser. 753 112014

(http://iopscience.iop.org/1742-6596/753/11/112014)

Comparing the Brushless DFIM to other Generator Systems for Wind Turbine Drive-Trains

Tim D. Strous, Udai Shipurkar, Henk Polinder and Jan A. Ferreira
Delft University of technology, Department of Electrical Sustainable Energy, Delft, The Netherlands

E-mail: t.d.strous@tudelft.nl

Abstract. In this paper, the brushless DFIM based wind turbine drive-train topology is compared to the DFIG based and PM generator based drive-train topologies, that are most commonly applied in modern wind turbines. The comparison will be based on a 3.2 MW case study wind turbine. By using FE based multi-objective optimization, optimized generator designs for the different topologies are generated. Then the capital expenditures of the resulting drive-train topologies are calculated and compared. Additionally, wind turbine drive-train configurations with 1, 2 and 3 stage gearboxes as well as a direct-drive configuration are taken into account. The resulting comparison shows that the brushless DFIM based drive-train with a 2 stage gearbox configuration provides a feasible alternative in commercial wind turbine drive-train applications.

1. Introduction

The wind energy market has shown a rapid growth over the last decades. In 1990, the total worldwide installed capacity was only 2.4 GW, but at the start of the new century, this amount had been ten folded and was still increasing, resulting in a total installed capacity of 370 GW by the end of 2014 [1]. Not only the wind energy market but also wind turbine technology and the applied wind turbine drive-train systems have been further developed, resulting in larger wind turbines with more efficient drive-train systems. Many modern wind turbines have either a PM generator system or a DFIG system at their core, but many alternative systems are currently investigated [2]. One alternative system that has gained a lot of research interest in recent years is the brushless Doubly-Fed Induction Machine (DFIM) [3]. This machine type has comparable operating characteristics to the conventional DFIG but has the additional advantage of increased robustness and reliability due to the absence of brush gear and slip rings. Because this is a low-speed machine type, the number of gearbox stages could be reduced, which increases system reliability even further.

The brushless DFIM houses two sets of stator windings, referred to as the power- and control-winding. The power-winding with p_p pole-pairs is directly connected to the grid. The control-winding with p_c pole-pairs is connected to a partially rated Power Electronic (PE) converter, enabling operation over a limited speed range. Both stator windings are (magnetically) indirectly coupled via a special rotor with a nested-loop construction [4]. The brushless DFIM operating principles and behaviour are more complex compared to more conventional generator systems. Recent research regarding the brushless DFIM has mainly focussed on providing insight into the brushless DFIM's operating principles, the development of accurate modelling techniques

and the development of control strategies. Brushless DFIM models have been developed using both analytical methods [5,6] and Finite Element (FE) techniques [7,8]. Because of those advances, it is now possible to develop optimized brushless DFIM designs for specified applications, using FE modelling and multi-objective optimization techniques.

The aim of this paper is to compare the brushless DFIM based wind turbine drive-train topology to the DFIG based and PM generator based drive-train topologies, in terms of Capital Expenditure (CapEx) cost. Comparisons of existing wind turbine drive-train topologies have been performed before. References [2,9–11] all show qualitative comparisons of existing generator systems, showing the strengths and weaknesses of those systems. In [12] a reliability comparison is performed, covering the components used in different wind turbine drive-train topologies. In yet another research an attempt was made to make a quantitative comparison of current generator systems in terms of energy yield and Capital Expenditure (CapEx) cost [13]. Since the performance of a wind turbine generator system depends on many factors, which can also change over the years (like the material cost for example), a clear 'best' generator system did not result from the aforementioned research results. This conclusion is also stressed by the variety of wind turbine generator systems produced and developed by the industry sector. Nevertheless, performing a CapEx cost comparison of wind turbine drive-train topologies that include the brushless DFIM system, will provide a good indication of the feasibility of commercializing such a system.

The executed wind turbine drive-train comparison in this paper is based on a case study wind turbine. By using FE based multi-objective optimization, optimized generator designs for the different topologies are generated. Then the CapEx cost of the resulting wind turbine drive-trains are calculated and compared. Additionally, generators are designed and compared for wind turbine drive-train topologies with varying gearbox stages. Resulting in a comparison of wind turbine drive-train topologies with 1, 2 and 3 stage gearboxes and a direct drive configuration for the PM generator based topology.

2. The Case-study Wind Turbine

For comparison of the different wind turbine drive-train topologies, a case-study wind turbine is used as a starting point. The wind turbine selected for the case-study is based on the Senvion 3.2M114 wind turbine with 3.2 MW rated power at 12.1 rpm rated speed. Further characteristics are provided in Table 1. Figure 1 provides a picture of the wind turbine.

The DFIG and PM generator based wind turbine drive-train topologies are most commonly applied in modern wind turbines. Therefore, they provide a solid reference for comparison to the brushless DFIM based wind turbine drive-train topology. These three different topologies are schematically presented in Figure 2. Aside from the applied generator systems, the drive-train

Figure 1: Senvion 3.2M114 Wind Turbine.

Table 1:
Wind Turbine Characteristics

Rated grid power	P_{rated}	3.2 MW
Rated wind speed	v_{wind}	12 m/s
Cut-in wind speed	v_{in}	3 m/s
Cut-out wind speed	v_{out}	22 m/s
Rotor diameter	D_{rotor}	114 m
Rated rotor speed	n_{WT}	12.1 rpm
Grid frequency	f_e	50 Hz

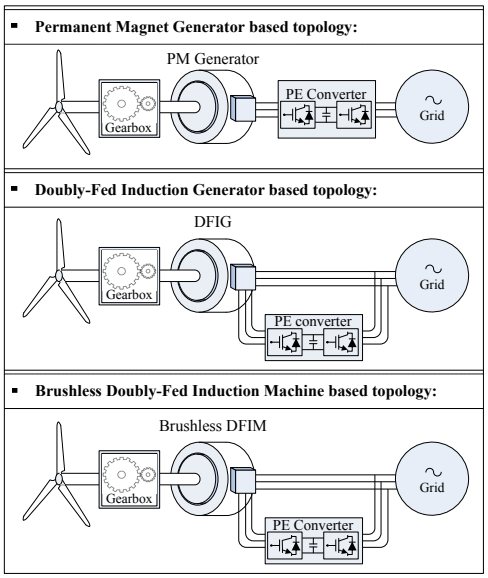

Figure 2: Wind Turbine Drive-Train topologies.

Table 2:
Wind Turbine Drive-Train Topologies

		PMG	**DFIG**	**BDFIM**
WT speed n_{WT} (rpm)		3 - 12.1	6 - 12.1	6 - 12.1
PE frequency f_c(Hz)		12 - 50	20 - (-10)	20 - (-10)
Gearbox		Generator		
Stages:	**Ratio r_{gear}:**	**Pole-pairs:**		
0	1 ($f_c = 4 - 16Hz$)	80	x	x
1	10	24	30	12, 18
2	30	8	10	4, 6
3	80	3	4	x

topologies differ by their applied PE converter. The PM generator based topology employs a fully rated PE converter, providing speed control over the entire wind turbine operating speed range. The DFIG and brushless DFIM based topologies, on the other hand, are equipped with a 30% partially rated PE converter, enabling speed control over a limited speed range, while keeping a speed margin for dynamic control in consideration. In this case speed range is sacrificed to reduce the cost of PEs. Additionally, for each drive-train topology, the number of gearbox stages can differ. More gearbox stages result in higher gearbox ratios and hence smaller generators, but at the expense of increasing gearbox cost.

This paper compares each selected drive-train topology with three different gearboxes. The selected gearboxes include a 1 stage gearbox with gear-ratio 10, a 2 stage gearbox with gear-ratio 30 and a 3 stage gearbox with gear-ratio 80. Additionally, a direct drive PM generator topology is taken into consideration. The brushless DFIM topology with 3 stage gearbox is not considered since this would yield non-practical brushless DFIM designs as will be explained later on.

The selected gear ratios r_{gear} also influences the number of pole-pairs p required for the selected generator in the wind turbine drive-train. The number of pole-pairs for each generator system is calculated according to:

$$\begin{aligned} PMgen. \;\Rightarrow\; p &= round\left(\frac{60\, f_c}{n_{WT}\, r_{gear}}\right) \\ DFIG \;\Rightarrow\; p &= round\left(\frac{60\,(f_e - f_c)}{n_{WT}\, r_{gear}}\right) \\ BDFIM \Rightarrow p_p + p_c &= round\left(\frac{60\,(f_e - f_c)}{n_{WT}\, r_{gear}}\right) \end{aligned}$$

Here f_e and f_c are respectively the grid frequency and the controllable PE converter frequency at nominal operation and n_{WT} is the rated wind turbine rotor speed. An overview of the different characteristics of each wind turbine drive-train topology used in this comparison study is presented in Table 2.

Direct drive configurations for DFIG and brushless DFIM topologies would result in unfeasible large generator designs and are therefore not considered. A brushless DFIM topology with a 3 stage gearbox is only possible if the selected number of pole-pairs are $p_p = 1$ and $p_c = 2$.

This specific selection of pole-pair numbers would result in generator designs with excessive unbalanced magnetic pull and harmonic related distortions and is therefore considered unfeasible to take into consideration for this comparison [8].

For each wind turbine drive-train topology as considered in Table 2 an optimized generator needs to be designed. The generator design optimization process will be discussed in the next section.

3. Generator Design Optimization

This paper compares different generator systems, with different gearbox configurations for wind turbine drive-trains in terms of CapEx cost. For this purpose, generators will be designed using multi-objective FE based optimization techniques. This allows determining a Pareto optimal front of generator designs for each generator configuration, showing a trade-off between efficiency and generator cost. An optimal generator design is then picked from the Pareto front for each wind turbine drive-train topology. The applied optimization procedure is first explained in section A. Then section B elaborates on the generator design modelling. Lastly, section C presents the optimization results of the generator designs for the different wind turbine drive-train topologies, as were presented in Table 2.

3.1. Optimization Procedure

Generator designs will be optimized, with efficiency and cost as optimization objectives. Generator cost is determined based on the cost price of used active materials and their corresponding mass. This includes the cost of copper, aluminium, magnet material and iron laminations. The total generator cost is therefore related to the generators mass. The applied optimization procedure in this paper is based on the FE based multi-objective optimization method presented in [8] and is schematically presented in Figure 3. The method uses the NSGA-II (non-dominated sorting genetic algorithm II [14]) optimization algorithm to determine a Pareto optimal front of generator designs.

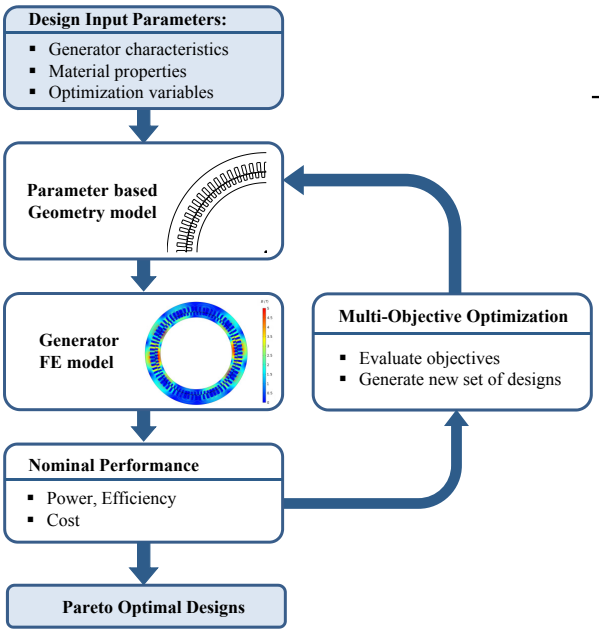

Figure 3: Generator design optimization procedure.

Table 3:
Modelling Characteristics

Generator Characteristics		
Number of phases	N_{ph}	3
Current density	J	4 A/mm^2
Winding distribution		Integer pitch
Slots per pole per phase	q	1-3
Slot fill factor	k_{fill}	0.6
Stator/rotor tooth tip height		$1/16^{th}$ tooth height
Stator/rotor tooth tip width		50% closed
Material Properties		
PM Remanent flux density	B_r	1.2 T
PM Coercive field strength	H_c	950 kA/m
Steel stacking factor	k_s	0.95
Eddy current loss constant	k_e	0.479
hysteresis loss constant	k_h	273
hysteresis loss constant 1	$k1$	1.256
hysteresis loss constant 2	$k2$	1.685
Generator Cost Modelling		
Cost-price of copper	C_{cu}	15 €/kg
Cost-price of steel	C_{Fe}	3 €/kg
Cost-price of magnets	C_{NdFeB}	60 €/kg
Cost-price of aluminium	C_{cu}	5 €/kg

Table 3 provides an overview of fixed modelling characteristics that are used during the optimization of the varying generator designs for the different wind turbine drive-train topologies. Those modelling characteristics, including generator characteristics and material properties, are used as input for the generator design optimization routine. First an initial population of N generator designs is evaluated. Each design varies based on a set of given variable geometric input parameters V. The design starts by determining the complete machine geometry using a parameter based geometry model developed in Matlab. Next, the generator geometry and additional input parameters, containing the nominal generator operating conditions, are transferred to Comsol via a Matlab-Comsol interface. Comsol is a FE program that determines the magnetic field distribution within the generator. By using post-processing the generator cost and performance in terms of output power and efficiency are determined and evaluated by the optimization algorithm in Matlab. Then a new generation of N generator designs is generated from the most optimal (fittest) individuals of the previous generation. Table 4 provides an overview of the optimization algorithm parameters, optimization variables and constraints that are used during the optimization of the different generator designs.

3.2. Generator Design Modelling

All generator designs considered during the optimization are evaluated using a 2-dimensional FE model generated in Comsol. Evaluating generator designs using FE analysis is more time consuming, though it yields more accurate results compared to analytical methods since non-linear effects such as iron saturation are more thoroughly taken into account. This is especially important for the brushless DFIM generator designs, which operate with two stator magnetic field components rotating at different speeds. Taking saturation accurately into account using analytical methods is therefore much more challenging [15].

The FE model of each design simulates the generator operating at its nominal operating speed for $1/4^{th}$ of a grid frequency time-period, $T = 0.005s$. Since the generator is modelled during stable synchronous operation, all stator windings are modelled as current sources rather than voltage sources. Each winding will be supplied with a nominal rms current density of $J = 4A/mm^2$. The FE solver determines the magnetic vector potential A_z (in the axial z-direction) within the generator, from which the 2-dimensional flux density distribution can be derived. The brushless DFIM FE model differs from the other two machine types in that it has a rotor nested-loop construction where currents are induced. The rotor currents $i_{r,l}$ in the different loops l are derived using Kirchoff's voltage law [7]:

Table 4:
Generator Design Optimization

Optimization Settings			**Geometric Optimization Variables**		**min**	**max**
Method		NSGA-II	Stator outer radius	r_{so}	0.5 m	3 m
Objectives		2			(For Direct Drive: max 5 m)	
Variables	V	8	Rotor inner radius	r_{ri}	$0.1 \cdot r_{so}$	$0.9 \cdot r_{so}$
Constraints		2	Stator inner radius	r_{si}	r_{ri}	r_{so}
Population size	N	50	Axial stack length	l_{stk}	0.3 m	3 m
Generations		20	Ratio stator slot/stator height	$\alpha_{s,y}$	0.2	0.8
Calc. time per gen.		38 $min.$	Ratio rotor (slot or PM)/rotor height	$\alpha_{r,y}$	0.2	0.8
FE elements per design		± 20e3 quadratic	Ratio stator inner/max slot width	$\alpha_{s,sw}$	0.2	0.8
			Ratio rotor inner/max slot width	$\alpha_{r,sw}$	0.2	0.8

Optimization Constraints
Tooth height ≤ 5·Tooth width
$P_e \geq P_{rated}$

$$i_{r,l}R_{r,l} = -\frac{l_{stk}}{S_{rl}}\frac{d}{dt}\left(\iint A_z dS_{rl+} - \iint A_z dS_{rl-}\right) \quad (1)$$

Here S_{rl+} and S_{rl-} are respectively the rotor loop 'go' and 'return' conductors and $R_{r,l}$ is the respective rotor loop resistance. Equation (1) is coupled with the field equations in the FE solver to solve the induced rotor currents iteratively.

The electromagnetic torque T_e generated by each generator is derived from the air-gap magnetic field using Maxwell's stress tensor method:

$$T_e = \frac{l_{stk}}{\mu_0} r_g^2 \int_0^{2\pi} B_r B_{tan} d\theta \quad (2)$$

Here B_r and B_{tan} are the radial and tangential components of the flux density in the air-gap at radius r_g and are derived from the magnetic vector potential according to:

$$B_r = \frac{\partial A_z}{r_g \partial\theta};\ B_{\tan} = -\frac{\partial A_z}{\partial r_g} \quad (3)$$

Equation (2) is used to derive the nominal electromagnetic power P_e that the generator generates.

Next, the different loss components during nominal operation are considered. These loss components include the copper and iron losses, which are derived in order to determine the generator designs efficiency:

$$\eta_{gen} = \frac{P_e - P_{cu,loss} - P_{Fe,loss}}{P_e} \cdot 100\% \quad (4)$$

The copper losses $P_{cu,loss}$ are derived by integrating the current density J_z over the area S_{cu} of the copper conductors:

$$P_{cu,loss} = \frac{l_{stk}\rho_{cu}}{k_{fill}} \iint J_z dS_{cu} \quad (5)$$

The iron losses $P_{Fe,loss}$ in the generator are calculated using a modified Steinmetz equation to determine the losses in different regions of the generator. The Eddy current losses, as well as the hysteresis losses in both the stator and rotor yoke and teeth sections, are calculated according to [16]:

$$\begin{aligned} P_{Fe,loss} = {} & \underbrace{k_e {f_e}^2 \left(\hat{B}_{ST}^2 V_{ST} + \hat{B}_{SY}^2 V_{SY}\right)}_{Stator\ Eddy\ current Losses} + \underbrace{k_e {f_r}^2 \left(\hat{B}_{RT}^2 V_{RT} + \hat{B}_{RY}^2 V_{RY}\right)}_{Rotor\ eddy\ current\ losses} \\ & + \underbrace{k_h f_e^{k_1} \left(\hat{B}_{ST}^{k_2} V_{ST} + \hat{B}_{SY}^{k_2} V_{SY}\right)}_{Stator\ hysteresis\ losses} + \underbrace{k_h f_r^{k_1} \left(\hat{B}_{RT}^{k_2} V_{RT} + \hat{B}_{RY}^{k_2} V_{RY}\right)}_{Rotor\ hysteresis\ losses} \end{aligned} \quad (6)$$

Here, V represents the volume of the respective area, while $\hat{B}$ represents the magnetic flux density peak value within the respective area. k_e and k_h are respectively the eddy current and hysteresis loss factors and $k1$ and $k2$ are material dependent constants. Equation (6) is slightly different for each considered generator type. Since higher order harmonic losses are neglected there will be no rotor losses considered for the PM generator types. Because the brushless DFIM

has two stator windings the eddy current losses and hysteresis losses in the stator are calculated differently from the other machine types:

$$\begin{aligned} P_{EC,loss} &= k_e \left({f_p}^2 \hat{B}_{PT}^2 + {f_c}^2 \hat{B}_{CT}^2 \right) V_{ST} + \left({f_p}^2 \hat{B}_{PY}^2 + {f_c}^2 \hat{B}_{CY}^2 \right) V_{SY} \\ P_{Hys,loss} &= k_h {f_p}^{k1} \left(\sqrt{\hat{B}_{PT}^2 + \hat{B}_{CT}^2} \right)^{k2} V_{ST} + k_h {f_p}^{k1} \left(\sqrt{\hat{B}_{PT}^2 + \hat{B}_{CT}^2} \right)^{k2} V_{SY} \end{aligned} \quad (7)$$

The power-winding and control-winding main magnetic field peak flux density values $\hat{B}_p$ and $\hat{B}_c$ are obtained through Fourier analysis of the magnetic field distribution using the method described in [7].

Lastly, the cost C_{gen} of the active materials used for a generator design is calculated according to:

$$C_{gen} = \rho_{Fe} V_{Fe} C_{Fe} + \rho_{cu} V_{cu} C_{cu} + \rho_{NdFeB} V_{NdFeB} C_{NdFeB} + \rho_{Al} V_{Al} C_{Al} \quad (8)$$

Here ρ is the mass density of the respective material, V is the volume of the respective material used in the generator design and C is the cost-price (in €/kg) of the respective material, which includes both material and labour costs. The rare earth neodymium (NdFeB) magnets are only applied for the PM generator designs while aluminium is only used for the brushless DFIM rotor nested-loop constructions.

3.3. Optimization Results

By using the optimization procedure and generator design models as described in sections 3.1 and 3.2, optimizations have been executed for the different generator types applied in the 3.2 MW wind turbine and for wind turbine drive-train topologies with varying number of gearbox stages. The resulting Pareto optimal fronts are presented in Figure 4, displaying the trade-off between generator design cost and efficiency. Figure 4 (a) shows the optimization results for the DFIG based wind turbine drive-train topologies, with a varying number of gearbox stages. Figures 4 (b) and (c) present the generator design optimization results for respectively the PM generator and brushless DFIM systems. The generator design optimization results for the direct-drive configuration are included in Figure 4 (d). For each wind turbine drive train topology, a single generator design is selected and will be used for the wind turbine drive-train comparison study. The selected generators are marked by the grey diamonds in Figure 4. The comparison of the varying wind turbine drive-train topologies with their optimized generator designs will follow in the next section.

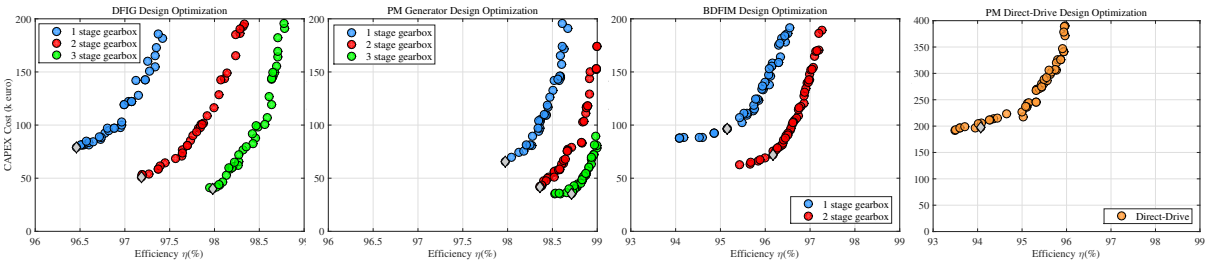

(a) (b) (c) (d)

Figure 4: Generator design optimization results for a 3.2 MW wind turbine drive-train

The optimization results clearly show a trend of cheaper (smaller) and more efficient designs with an increased number of gearbox stages and hence increased gear ratios and generator speeds. This is as could be expected. The cost of active material for the DFIG designs is approximately 20% higher than for the PM generator designs (considering equal gear stages). The brushless DFIM designs are heavier, more costly and less efficient than both of those design variations. Though, the difference in price between DFIGs and brushless DFIMs is lower than expected when considering their difference in mass. It is the application of aluminium, instead of copper, for the rotor bars that reduces the difference. The same goes for the PM generator designs with their relatively high PM material cost price, that drives up the price of the PM generators more than would be expected based on a mass comparison. Additionally, the PM material cost-price is prone to price fluctuations over the years, making the investment in large-scale PM generators riskier. PM generators seem to have the edge over the DFIGs in terms of efficiency, but it needs to be considered if this will still hold when considering efficiency on a system level.

4. Wind Turbine Drive-Train Comparison

This section compares the PM generator, DFIG and brushless DFIM based wind turbine drive-train topologies, with varying gearbox stages (and ratios), in terms of nominal efficiency performance and CapEx cost. A comparison overview is presented in Table 5. The first section of Table 5 shows the differences of the drive-train topologies in terms of applied gearbox stages, gearbox r atios and selected number of generator pole-pairs. For each topology, an optimized generator design is selected from the optimization results presented in section 3. The resulting generator design dimensions and masses of used materials are shown in respectively sections two and three of Table 5.

Here the generator housing mass is assumed to be equal to the sum of the weight of the used active materials.

The fourth section covers the nominal efficiency of the different drive-train components. The gearbox efficiency at rated operating speed is considered to be 98.5% for a single stage gearbox minus 1% efficiency for each additional gear stage. The efficiency of a fully rated PE converter is considered to be 97% at rated operating speed. For the partially rated converters, the efficiency is 99% based on the PE converter losses and the fully rated drive-train power. The generator designs from section 3 were selected in such a manner that the total system efficiency during nominal operation was approximately equal between 91% and 94%.

The last section of Table 5 compares the drive-train CapEx cost, considering the cost of the generator gearbox and PE converter. Here it is assumed that a 3 MW single stage gearbox costs €150.000,-, with an additional cost of €35.000,- for each additional gearbox stage. The PE cost is considered to be 40€/kW. The generator housing cost is considered to be approximately equal to the generators total active material cost.

From the results, it appears that wind turbine drive-train systems with 2 stage gearboxes are favourable over drive-train systems with other gearbox configurations. This result is independent of the selected generator type. Further, the results demonstrate that DFIG based wind turbine drive-train systems provide the lowest cost solutions in terms of CapEX costs. The highest system cost, on the other hand, can be attributed to the PM generator drive-train systems. This can be explained by the increased cost of the PE converters. However, since the cost of PEs is declining over the years, the PM generator drive-train systems are a competitive alternative to keep into consideration. It is interesting to see that the brushless DFIM drive-train systems are only 10% more expensive in terms of CapEx costs, compared to the DFIG drive-train systems and that they are less costly compared to the PM generator drive-train systems. However, the brushless DFIM has some additional advantages over the conventional DFIG, especially with regards to reliability and maintenance issues. The effects of those advantages on the operational expenditures and therefore on the total system cost and revenue over its lifetime, are

Table 5:
Wind Turbine Drive-Train Topologies Comparison

	Wind Turbine Drive-Train Characteristics								
Generator system:	**PM Generator**				**DFIG**			**Brushless DFIM**	
Gearbox stages:	0	1	2	3	1	2	3	1	2
Gearbox ratio r_{gear}:	1	10	30	80	10	30	80	10	30
Generator pole-pairs:	80	24	8	3	30	10	4	12, 18	4, 6
	Generator Design Dimensions								
Number of stator slots:	480	144	48	18	360	120	72	216	72
Number of rotor slots:	0	0	0	0	180	60	48	240	80
Air-gap length $l_g(mm)$:	8.8	3.8	2.6	2.6	5.7	2.6	2.6	3.8	2.6
Stack length $l_{stk}(m)$:	0.49	0.25	0.59	0.48	0.3	0.5	0.55	0.63	0.51
Stat. out. rad. $r_{so}(m)$:	4.53	2.08	0.91	0.52	3	1.28	0.72	2.04	1.36
Stat. in. rad. $r_{si}(m)$:	4.39	1.91	0.76	0.35	2.83	1.12	0.54	1.89	1.05
Rot. in. rad. $r_{ri}(m)$:	4.33	1.83	0.66	0.21	2.69	0.95	0.32	1.70	0.85
	Generator Design Mass (ton)								
Generator steel:	14.10	4.16	4.45	1.73	10.65	7.24	4.28	14.34	11.47
Generator copper:	6.10	2.10	1.02	0.91	3.14	1.96	1.79	3.33	2.43
Generator PMs:	1.07	0.37	0.22	0.28	0	0	0	0	0
Generator aluminium:	0	0	0	0	0	0	0	0.68	0.28
Total generator:	21.26	6.62	5.69	2.92	13.79	9.21	6.07	18.35	14.19
	Wind Turbine Drive-Train Nominal Efficiency (%)								
Generator:	94.1	98.0	98.4	98.7	96.5	97.2	98.0	95.2	96.2
Gearbox:	100	98.5	97.5	96.5	98.5	97.5	96.5	98.5	97.5
PE Converter:	97	97	97	97	99	99	99	99	99
Total Drive-train:	**91.1**	**93.5**	**92.9**	**92.2**	**94**	**93.7**	**93.5**	**92,7**	**92.7**
	Wind Turbine Drive-Train CapEx Cost (k€)								
Generator steel:	42.30	12.50	13.36	5.18	31.95	21.73	12.84	43.03	34.41
Generator copper:	91.34	31.43	15.24	1.37	47.06	29.42	26.91	49.91	36.46
Generator PMs:	64.47	21.94	13.33	16.91	0	0	0	0	0
Generator aluminium:	0	0	0	0	0	0	0	3.40	1.42
Generator housing:	198	66	42	36	80	51	40	96	72
Total generator:	**396.1**	**131.9**	**83.9**	**71.8**	**159.0**	**102.2**	**79.8**	**192.3**	**144.3**
Gearbox:	0	150	185	220	150	185	220	150	185
PE converter:	128	128	128	128	38.4	38.4	38.4	38.4	38.4
Total system:	**524.1**	**409.9**	**396.9**	**419.8**	**347.4**	**325.6**	**338.2**	**380.7**	**367.7**

not considered in this comparison study and need to be investigated separately. Nevertheless, the results form this study show that the brushless DFIM, together with a 2 stage gearbox, provides a feasible alternative for commercial wind turbine drive-train applications.

5. Conclusions

The brushless DFIM is an interesting generator system for wind turbine drive-trains. This paper compared the brushless DFIM to the DFIG and PM generator based wind turbine drive-train topologies with several different gearbox configurations. The drive-train topologies were compared based on CapEx cost, using a 3.2 MW wind turbine case-study. For each drive-train topology, an optimized generator design was selected from a set of Pareto optimal designs, generated using FE based multi-objective optimization design tools.

The generator design CapEx cost for the different generator types deviated less than what could be expected based on the difference in mass. The brushless DFIM generator type is the heaviest and most expensive, but the use of aluminium rotor bars reduces the difference in cost with the DFIG. On the other hand, the use of PMs inflates the CapEx cost of PM generators.

Still, the PM generator designs were more efficient and less costly compared to the other two generator types for drive-train systems with equal gearbox ratios.

Complete wind turbine drive-train system configurations were compared, including their optimized generator designs. The drive-train configurations with 2 stage gearboxes appeared favourable over other configurations. The PM generator based drive train systems and especially the direct-drive configuration seemed to yield the highest CapEx cost while the DFIG based drive-train systems appeared to be the most favourable in terms of CapEx cost. The brushless DFIM drive-train systems are only 10% more expensive compared to the DFIG drive-train systems, but considering their additional advantages they could provide a feasible alternative to commercial wind turbine drive-train applications.

References

[1] "Global wind report 2014 - annual market update," Global Wind Energy Council, Tech. Rep., 2014.
[2] H. Polinder, J. Ferreira, B. Jensen, A. Abrahamsen, K. Atallah, and R. McMahon, "Trends in wind turbine generator systems," *IEEE Journal of Emerging and Selected Topics in Power Electronics*, vol. 1, no. 3, pp. 174–185, 2013.
[3] R. A. McMahon, X. Wan, E. Abdi-Jalebi, P. Tavner, P. C. Roberts, and M. Jagiela, "The bdfm as a generator in wind turbines," in *12th Int. Power Electron. and Motion Control Conf., EPE-PEMC.*, 2006, pp. 1859–1865.
[4] E. Wiedenbrug, M. Boger, A. Wallace, and D. Patterson, "Electromagnetic mechanism of synchronous operation of the brushless doubly-fed machine," in *Conf. Rec. Ind. Applicat. IEEE 13th IAS Annual Meeting*, vol. 1, 1995, pp. 774–780.
[5] T. D. Strous, N. H. van der Blij, H. Polinder, and J. A. Ferreira, "Brushless doubly-fed induction machines: Magnetic field modelling," in *Int. Conf. Elect. Machines (ICEM)*, Sep. 2014, pp. 2702–2708.
[6] H. Gorginpour, H. Oraee, and R. McMahon, "A novel modeling approach for design studies of brushless doubly fed induction generator based on magnetic equivalent circuit," *IEEE Trans. Energy Convers.*, vol. 28, no. 4, pp. 902–912, 2013.
[7] X. Wang, T. D. Strous, D. Lahaye, H. Polinder, and J. A. Ferreira, "Finite element modeling of brushless doubly-fed induction machine (bdfim) based on magneto-static simulation," in *Int. Conf. Elect. Machines & Drives (IEMDC)*, May 2015, pp. 315–321.
[8] T. D. Strous, X. Wang, H. Polinder, and J. A. Ferreira, "Finite element based multi-objective optimization of a brushless doubly-fed induction machine," in *Int. Conf. Elect. Machines & Drives (IEMDC)*, May 2015, pp. 1689–1694.
[9] S. N. Mohammad, N. K. Das, and S. Roy, "A review of the state of the art of generators and power electronics for wind energy conversion systems," in *Developments in Renewable Energy Technology (ICDRET), 2014 3rd International Conference on the*, 2014, pp. 1–6.
[10] H. Li and Z. Chen, "Overview of different wind generator systems and their comparisons," *IET Renewable Power Generation*, vol. 2, no. 2, pp. 123–138, 2008.
[11] H. Polinder, "Overview of and trends in wind turbine generator systems," in *Power and Energy Society General Meeting, 2011 IEEE*, 2011, pp. 1–8.
[12] J. Carroll, A. McDonald, and D. McMillan, "Reliability comparison of wind turbines with dfig and pmg drive trains," *IEEE Trans. Energy Convers.*, vol. 30, no. 2, pp. 663–670, 2015.
[13] H. Polinder, F. van der Pijl, G.-J. de Vilder, and P. Tavner, "Comparison of direct-drive and geared generator concepts for wind turbines," *IEEE Trans. Energy Convers.*, vol. 21, no. 3, pp. 725–733, 2006.
[14] K. Deb, A. Pratap, S. Agarwal, and T. Meyarivan, "A fast and elitist multiobjective genetic algorithm: NSGA-II," *IEEE Trans. Evol. Comput.*, vol. 6, no. 2, pp. 182–197, 2002.
[15] T. D. Strous, X. Wang, H. Polinder, and A. Ferreira, "Saturation in brushless doubly-fed induction machines," in *to be presented at IET Int. Conf. Power. Electron. Machines Drives (PEMD)*, 2016.
[16] H. Gorginpour, H. Oraee, and E. Abdi, "Calculation of core and stray load losses in brushless doubly fed induction generators," *IEEE Trans. Ind. Electron.*, vol. 61, no. 7, pp. 3167–3177, 2014.